2-μm 1.5-W Optically Pumped Semiconductor Membrane Laser

Maximilian C. Schuchter, Nicolas Huwyler, Matthias Golling, Marco Gaulke, and Ursula Keller, *Fellow, IEEE*

***Abstract*— We introduce the first diode-pumped GaSb-based semiconductor membrane laser with a continuous wave (cw) output power of 1.5 W at a center wavelength of 2.08 μm with an optical-to-optical efficiency of 11.7 % and thermal resistance of 0.74 K/W. It features a broad tunability over 117 nm, achieved using a 3-mm birefringent quartz crystal in Brewster configuration. This tuning range is currently limited by the dielectric cavity mirrors. The laser beam quality, indicated by an $M^2 < 1.45$, remains excellent across all output powers. Unlike diode-pumped ion-doped solid-state lasers, this semiconductor laser offers full wavelength flexibility through InGaSb quantum well (QW) bandgap engineering in the short-wave-infrared (SWIR) regime. The 1.2-μm thick membrane gain chip with 12 InGaSb QWs is directly bonded on a silicon carbide heatspreader. This type of laser is also referred to as a MECSEL (Membrane External Cavity Surface Emitting Laser) which can support high-power operation in the SWIR regime due to their excellent heat dissipation. We developed new processing techniques to showcase the promising results for MECSEL in the GaSb-based material system.**

***Index Terms*— GaSb, MECSEL, VECSEL, SESAM, semiconductor lasers, cw-lasing, short-wave-infrared, DBR-free.**

I. Introduction

OPTICALLY pumped GaAs-based semiconductor lasers have replaced Ti:sapphire lasers for many commercial bio-medical applications. In contrast to electrically pumped semiconductor lasers high-power operation above 100 W in the near-infrared can be obtained with optical pumping [1]. The AlAs/GaAs Distributed Bragg Reflector (DBR) has a small lattice mismatch, high refractive index contrast to obtain high reflectivity with a small number of layer pairs. Integration of such a DBR with a gain section resulted in the first diode-pumped vertical external cavity surface emitting laser (VECSEL) [2]. This laser platform was used to expand into the visible and short-wave-infrared (SWIR) regime offering low-noise high-power and tunable single frequency operation with excellent beam quality [3]. Passively modelocked VECSELs [4] have been achieved with semiconductor saturable absorber mirrors (SESAMs) and full integration of VECSEL and SESAM layers into one semiconductor chip, referred to as the MIXSEL (Modelocked Integrated eXternal-cavity Surface Emitting Laser) [5] with reduced complexity and supporting pulse repetition rates scaling up to 100 GHz [6]. The MECSEL (Membrane External Cavity Surface Emitting Laser) [7], [8] further simplifies optically pumped semiconductor lasers with removing the DBR and leaving only a thin gain membrane to support operation wavelength spanning from 600 nm to 1.75 μm [7], [9] using both the GaAs and InP material system. Additionally it addresses the thermal [10] and refractive-index-contrast limitations, like in InP-based DBRs, which are present in traditional VECSEL configurations [11], and also supports record-wide wavelength tunability [12].

The success story of GaAs-based optically pumped semiconductor lasers motivated the work on GaSb-based lasers to expand the operation wavelength into the SWIR and mid-IR regime. VECSELs emitting in the 1.9 to 3 μm range are based on the GaSb material system. Devices operating in this range can benefit from the high index contrast of AlAsSb/GaSb DBRs, which on the other hand suffer from poor thermal conductivity (~8 times lower compared to AlAs/GaAs DBRs). However, the quantum defect reduction obtained using 1.45-μm pump diodes relaxes the heat load on the structures and allows for high-power cw operation at non-cryogenic temperatures. A 2.02 μm VECSEL with 10 InGaSb QWs and a double heatspreader technique generated a maximum cw power up to 20.7 W [13] and also 17 W at room temperature operation [14]. GaSb-based VECSELs have been modelocked [7] and high-quality InGaSb SESAMs [15] enabled shorter pulses and higher output power [16]. The thermal resistance for cw 2-μm VECSELs [17] could be reduced with a hybrid metal-semiconductor Bragg reflector [18]. More recently a GaSb-based MIXSEL has been demonstrated in single- and dual-comb operation [19].

Here we introduce the development of new processing techniques in the GaSb-based material system with the demonstration of a GaSb-based MECSEL at 2.08 μm. The MECSEL has a cw output power exceeding 1.5 W, a tuning range of 117 nm and a thermal resistance of 0.74 K/W with only a single heatspreader technique. A direct bonding process of a GaSb-based semiconductor chip to a SiC heatspreader was developed for this result.

II. Design, Fabrication and Experimental Setup

Figure 1a) shows the design of the epitaxial heterostructure of the MECSEL gain chip with a total thickness of 1.2 μm.

Manuscript received 23 January 2024; revised 27 February 2024; accepted 9 March 2024. Date of publication 13 March 2024; date of current version 22 March 2024. This work was supported by European Research Council (ERC) under European Union's Horizon 2020 Research and Innovation Program under Grant 787097. *(Corresponding author: Maximilian C. Schuchter.)*

Maximilian C. Schuchter is with the Ultrafast Laser Physics Group, Institute for Quantum Electronics, ETH Zürich, 8093 Zürich, Switzerland, and also with the Optoelectronics Research Centre (ORC), Physics Unit/Photonics, Faculty of Engineering and Natural Sciences, Tampere University, 33720 Tampere, Finland (e-mail: mschucht@phys.ethz.ch; maximilian.schuchter@tuni.fi).

Nicolas Huwyler, Matthias Golling, Marco Gaulke, and Ursula Keller are with the Ultrafast Laser Physics Group, Institute for Quantum Electronics, ETH Zürich, 8093 Zürich, Switzerland.

Color versions of one or more figures in this letter are available at https://doi.org/10.1109/LPT.2024.3377261.

Digital Object Identifier 10.1109/LPT.2024.3377261

A standard 2-μm VECSEL structure [17] in comparison, has a total thickness of 6.7 μm. The active region consists of 4 sets of 3 $In_{0.27}Ga_{0.73}Sb$ quantum wells (4 × 3 QWs), where each QW has a thickness of 8 nm. The QWs are placed within the antinodes of the lasing wavelength enhancing the efficiency of the lasing process and reducing threshold pump power. Carrier diffusion is managed by 10-nm thick GaSb layers serving as pump absorbers. Further confinement, preventing carrier run-away, is achieved using $AlAs_{0.08}Sb_{0.92}$ as cladding material. The design incorporates antiresonant closings on both sides, contributing to the stability and performance of the MECSEL [20]. The Molecular Beam Epitaxy (MBE) growth on an GaSb wafer was started with a 150-nm $InAs_{0.91}Sb_{0.09}$ layer which forms an etch stop for subsequent wafer removal. After MBE growth the MECSEL membrane gain chip is bonded onto a silicon carbide (SiC) heat spreader. Room temperature direct wafer bonding was developed for the GaSb material system to optimize thermal conductivity. A 6.5 × 6.5 mm MECSEL chip and 10 × 10 mm SiC heatspreader are cleaned with a methanol wipe and subsequently ultrasonic baths of acetone, isopropanol and methanol, following an O_2 plasma. The SiC substrates are chosen for their superior surface quality with very low micro roughness on the nm-scale of <0.2 nm rms. The bonding process to the heatspreader is the most crucial step in achieving a good MECSEL chip.

This requires a clean environment during the cleaning process with a particular focus on preventing dust and scratches on the sample. Any existing scratches may render the bonding ineffective, and the presence of dust particles can result in only partial bonding, leading to debonding during post-processing. To maintain a clean environment, the entire procedure is conducted in a cleanroom facility. Furthermore, the radius of curvature (R_{oc}) of the MECSEL samples were observed to play a significant role. A R_{oc} of less than 15 m or the presence of a saddle point in the MECSEL chip curvature reduces the likelihood of successful bonding. Additionally, improper cleaving can introduce strain effects, contributing to an increased curvature.

After bonding, the GaSb substrate is removed by lapping down to 20-40 μm followed by wet-etching the remaining substrate with a solution mixture of 33 % CrO_3 and 50 % hydrofluoric acid, diluted in water 1 : 5 [17]. The $InAs_{0.91}Sb_{0.09}$ etch stop is then removed with a solution of citric acid and hydrogen peroxide yielding the finished MECSEL chip on a single SiC heatspreader. At this point no anti-reflection (AR) coating was applied.

Figure 1b) shows a typical MECSEL membrane bonded onto a SiC substrate. It is crucial to highlight that inadequate bonding can lead to under etching during the etching process. In such cases, the etchant may flow into the interface between SiC and the membrane, resulting in debonding of the membrane. The MECSEL chip is placed within a water-cooled copper mount, temperature-controlled by a thermoelectric cooler (TEC) element. The entire assembly is mounted onto an XYZ stage, further situated on a tilt/jar stage. The copper heatsink temperature is stabilized between 10 - 20 degrees for all measurements, ensuring stable lasing across a range of temperatures.

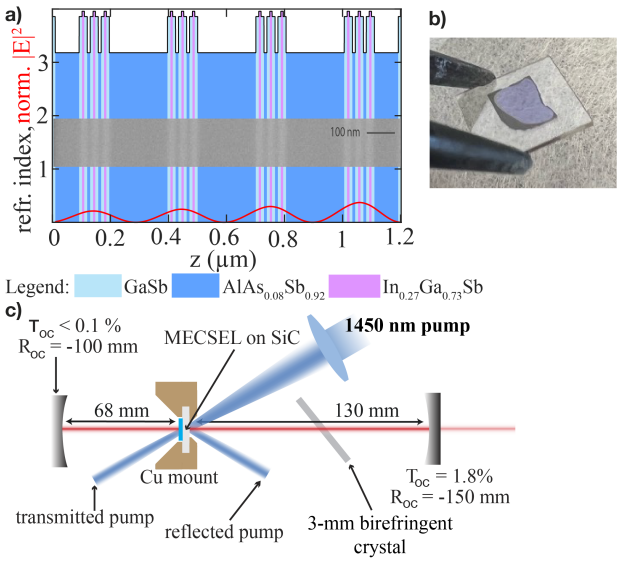

Fig. 1. MECSEL gain chip design and experimental setup. a) The resonant periodic gain quantum well (QW) arrangement in the active region displayed with the refractive index and simulated E-field intensity as a function of distance normal to the chip surface. A scanning electron microscope (SEM) image of the active region is laid over. b) A picture of a fully processed MECSEL chip using a single 10×10 mm SiC heatspreader. Tweezer tip for size comparison. c) Straight linear MECSEL cavity, containing a highly reflective mirror, with a −100 mm radius of curvature (R_{oc}) and an output coupler with a power transmission (T_{oc}) of 1.8 % and a R_{oc} of −150 mm. The 3-mm birefringent crystal is used to tune the MECSEL wavelength.

Figure 1c) depicts the final laser cavity with the optically pumped MECSEL chip. The straight linear MECSEL cavity contains two end mirrors: a highly reflective mirror (>99.9 %) between 2000-2100 nm with a $R_{oc} = -100$ mm, and an output coupler with 1.8 % power transmission and a $R_{oc} = -150$ mm. Respective distances between the cavity mirrors establish a lasing mode of 356 μm beam diameter on the MECSEL chip. For wavelength tuning a 3-mm birefringent quartz crystal is inserted at the Brewster angle. The pump laser is a 45-W Dilas laser diode emitting at 1450 nm with an $M^2 \approx 72$. The diode is collimated using a 75-mm lens and focused with a 50-mm lens, resulting in an elliptical spot on the MECSEL with a short-axis beam waist of 285 μm due to the 30-degree pump angle.

III. MECSEL Performance

A. CW Lasing

In Figure 2a), the free-running MECSEL's output power is depicted as a function of absorbed pump power across heatspreader temperatures ranging from 10 to 20 degrees. Given the absence of wavelength stabilization, the power is dispersed across multiple longitudinal modes, as illustrated in the inset, leading to fluctuations. The figure only shows 11 temperature powerslopes, whereas in the actual measurement we performed measurements in steps of 0.5 °C, giving in total 21 powerslopes. The figure inset shows a typical spectrum of the free-running MECSEL at a center wavelength of 2.08 μm. A maximum cw output power exceeding 1.5 W is achieved with no saturation. This demonstrates excellent power scaling capabilities in comparison to VECSELs [17]. Even at room temperature operation 20 °C, there is no thermal

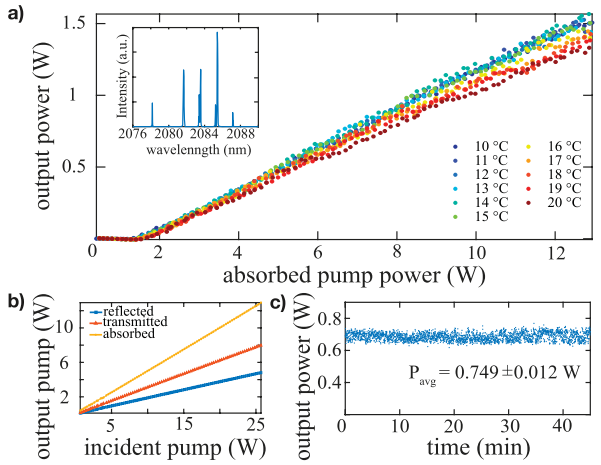

Fig. 2. CW lasing performance. a) The output power of the free-running MECSEL vs. absorbed pump power at different temperatures. The inset shows a typical spectrum of the free-running MECSEL around 2.08 μm. b) The absorbed (50.0 %), reflected (18.8 %), and transmitted (31.2 %) pump powers vs. incident pump power at 15 °C c) A power stability measurement of the MECSEL at 15 °C with 10 W absorbed pump power.

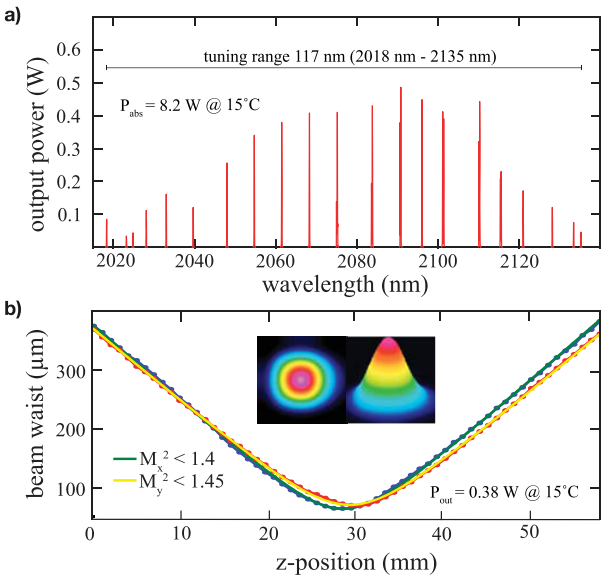

Fig. 3. Wavelength tuning and beam shape. (a) A tuning range of 117 nm with a 3-mm birefringent crystal in Brewster's angle configuration was achieved. The tuning curve was recorded at an absorbed pump power of 8.2 W at a MECSEL mount temperature of 15 °C and its intensity was normalized to the output power. Each spectral line was recorded at a different birefringent crystal position. (b) M^2 measurement compliant with the ISO 11146 standard, at an output power of 380 mW @ 15 °C. The collimated beam was focused into the M^2 stage via a 150-mm aspheric lens.

rollover due to the heat dissipation through the one-sided SiC heatspreader.

Figure 2b) shows the absorbed (50.0 %), reflected (18.8 %), and transmitted (31.2 %) pump power which results in an optical-to-optical efficiency of 11.7 % at 15 °C as a function of absorbed pump power. According to [17], a front-side cooled diamond top-heatspreader VECSEL chip demonstrates an optical-to-optical efficiency of 7.4 % at 17 °C as a function of incident pump power with a reflected pump below 7 %. Despite having only 4 × 3 InGaSb quantum wells, the MECSEL demonstrates a higher optical-to-optical efficiency. The thermal resistance, with calculations adapted from [11] and [18], is notably low at 0.742±0.16 K W^{-1}. This is a significant improvement compared to an upside-down grown hybrid mirror VECSEL soldered onto a diamond heatsink, which reported a thermal resistance of 2.12±0.19 K W^{-1} [18]. Additionally, we also beat the VECSEL cooled with a diamond top-heatspreader, which reported an up-to-date lowest thermal resistance of 0.97 K W^{-1} for 2-μm GaSb-based VECSELs [14]. This underscores the superior thermal management capabilities of MECSELs in comparison to VECSELs in the GaSb-based material system.

Internal losses are evaluated through different output couplers using the Finlay Clay method [21]. Using 4 different output couplers with 0.5 %, 1 %, 1.3 %, and 1.8 % power transmission, a linear fit through the output coupling rate over the threshold power yields the intracavity losses of $T_{ic,loss}$ = 3.7 % for the MECSEL. No literature exists on the intracavity losses of GaSb-based VECSELs. We anticipate these losses to be similar to those in AlGaInP VECSELs at around 660 nm, as noted in [22]. High-quality processing typically leads to lower intracavity losses.

Figure 2c) further illustrates the power stability of a free-running MECSEL at 10-W absorbed power and a heatsink temperature of 15 °C for 45 minutes, with average output power of 0.749±0.012 W. In this first GaSb-based MECSEL demonstration, we achieved cw-lasing performance comparable to prior VECSELs with superior heat dissipation.

B. Wavelength Tuning and Spatial Mode Quality

Wavelength tunability was explored with an intracavity 3-mm thick birefringent quartz crystal plate inserted at Brewster's angle. Rotating the crystal plate around its normal axis shifts the operation wavelength. Figure 3a) shows the tuning range measured with an optical spectrum analyzer (OSA) at various rotation positions of the birefringent crystal under constant absorbed pump power of 8.2 W and a constant heatsink temperature of 15 °C. The spectral lines were normalized to the laser output power. This results in a total tuning range of 117 nm, stretching from 2018 nm to 2135 nm. This corresponds to a tuning range of 8.16 THz. Figure 3a) also reveals that the highest gain is achieved at 2090 nm resulting in the maximum output power. From spectral gain simulations [17], we would not expect the limited tunability towards longer wavelengths. This effect can be explained by bandwidth constraints from the dielectric laser cavity mirrors. A high reflectivity of >99.9 % is only available between 2 and 2.1 μm and drops for longer wavelengths. This would suggest the potential for an even broader tuning range of this MECSEL gain chip. A VECSEL operating around 2 μm revealed a tuning range of 5.8 THz [23], whereas the broadest tuning range was achieved with a 1-μm MECSEL and a range of 26.5 THz [12]. However, this 1-μm MECSEL has been specifically optimized for broad tuning by using two different sets of quantum wells and optimizing their location within the standing wave intensity profile. In contrast, for our 2-μm MECSEL we used only one type of quantum well.

The beam quality assessment of the free-running MECSEL is conducted at an output power of P_{out} = 0.38 W and heatsink temperature of 15 °C. Figure 3b) presents the beam waist in x and y over the propagation distance z. The insets display the beam shape at the focusing point of the beam. The beam

waist over the z-propagation was measured using an extended InGaAs scanning slit profiler, coupled with a linear stage. In adherence to the ISO 11146 standard, the recorded beam quality factor M^2 was measured to be $M_x^2 = 1.38$ and $M_y^2 = 1.44$. The accuracy of the device in this assessment is within ± 2 %. In comparison, similar M^2 values for VECSELs and MECSELs at high power operation are shown in literature [8].

IV. Conclusion

In this study, we have achieved, to the best of our knowledge, the first MECSEL in the GaSb material system. The free-running MECSEL, with a center wavelength of 2.08 μm, marks a significant milestone result in extending MECSEL technology into the SWIR regime. Our experiments demonstrate the feasibility of room-temperature operation with a slope efficiency comparable to commercially available VECSELs at this wavelength [17], all achieved without encountering thermal rollover. For previous GaSb-based VECSELs the thermal rollover has often been a limiting factor. We demonstrated a broad tunning range from 2018 nm to 2135 nm (i.e. 117 nm, 8.2 THz) currently limited in the long wavelength regime by the dielectric laser cavity mirrors. This tuning range can be further optimized using different quantum wells distributed at different positions within the standing wave profile. The quality of direct wafer bonding between the heatspreader and membrane, as well as substrate removal via lapping and HF etching, play pivotal roles in thermal resistance and surface quality [11]. The prospect of bonding a second heatspreader onto the processed MECSEL chip surface is expected to further improve the thermal resistance. As demonstrated with GaAs-based MECSELs we can expect further performance improvements of the GaSb-based MECSELs with AR coatings on the heat spreaders and double-side pumping.

This GaSb-based MECSEL overcomes the thermal limitations of thick DBRs in the longer wavelength regime, enabling high-power operation. Its short MBE growth runs reduce propagation defects typical in longer runs, preserving crystal integrity. Our results presented here make GaSb-based MECSELs a promising candidate for expanding operational wavelengths, possibly by employing both type-I and type-II quantum wells.

Acknowledgment

The authors would like to thank the FIRST clean room facility at ETH Zurich and Open AI's ChatGPT-3.5 version acting as an English language editing service. They acknowledge helpful discussions with Hermann Kahle and Mircea Guina.

References

[1] B. Heinen et al., "106 W continuous-wave output power from vertical-external-cavity surface-emitting laser," *Electron. Lett.*, vol. 48, no. 9, p. 516, 2012, doi: 10.1049/el.2012.0531.

[2] M. Kuznetsov, F. Hakimi, R. Sprague, and A. Mooradian, "High-power (>0.5-W CW) diode-pumped vertical-external-cavity surface-emitting semiconductor lasers with circular TEM_{00} beams," *IEEE Photon. Technol. Lett.*, vol. 9, no. 8, pp. 1063–1065, Aug. 1997.

[3] M. Guina, A. Rantamäki, and A. Härkönen, "Optically pumped VECSELs: Review of technology and progress," *J. Phys. D, Appl. Phys.*, vol. 50, no. 38, Sep. 2017, Art. no. 383001, doi: 10.1088/1361-6463/aa7bfd.

[4] B. W. Tilma et al., "Recent advances in ultrafast semiconductor disk lasers," *Light, Sci. Appl.*, vol. 4, no. 7, p. 310, Jul. 2015, doi: 10.1038/lsa.2015.83.

[5] D. J. H. C. Maas et al., "Vertical integration of ultrafast semiconductor lasers," *Appl. Phys. B, Lasers Opt.*, vol. 88, no. 4, pp. 493–497, Sep. 2007, doi: 10.1007/s00340-007-2760-1.

[6] M. Mangold, C. A. Zaugg, S. M. Link, M. Golling, B. W. Tilma, and U. Keller, "Pulse repetition rate scaling from 5 to 100 GHz with a high-power semiconductor disk laser," *Opt. Exp.*, vol. 22, no. 5, p. 6099, Mar. 2014, doi: 10.1364/oe.22.006099.

[7] Z. Yang, A. R. Albrecht, J. G. Cederberg, and M. Sheik-Bahae, "Optically pumped DBR-free semiconductor disk lasers," *Opt. Exp.*, vol. 23, no. 26, p. 33164, Dec. 2015, doi: 10.1364/oe.23.033164.

[8] H. Kahle et al., "Semiconductor membrane external-cavity surface-emitting laser (MECSEL)," *Optica*, vol. 3, no. 12, p. 1506, Dec. 2016, doi: 10.1364/OPTICA.3.001506.

[9] A. Broda, B. Jeżewski, I. Sankowska, M. Szymański, P. Hoser, and J. Muszalski, "Growth and characterization of InP-based 1750 nm emitting membrane external-cavity surface-emitting laser," *Appl. Phys. B, Lasers Opt.*, vol. 126, no. 12, p. 192, Dec. 2020, doi: 10.1007/s00340-020-07544-y.

[10] H.-M. Phung et al., "Thermal behavior and power scaling potential of membrane external-cavity surface-emitting lasers (MECSELs)," *IEEE J. Quantum Electron.*, vol. 58, no. 2, pp. 1–11, Apr. 2022, doi: 10.1109/JQE.2022.3147482.

[11] M. Devautour, A. Michon, G. Beaudoin, I. Sagnes, L. Cerutti, and A. Garnache, "Thermal management for high-power single-frequency tunable diode-pumped VECSEL emitting in the near- and mid-IR," *IEEE J. Sel. Topics Quantum Electron.*, vol. 19, no. 4, Jul. 2013, Art. no. 1701108, doi: 10.1109/JSTQE.2013.2245104.

[12] P. Rajala et al., "Multi-type quantum well semiconductor membrane external-cavity surface-emitting lasers (MECSELs) for widely tunable continuous wave operation," 2023, *arXiv:2309.05409*.

[13] P. Holl et al., "Recent advances in power scaling of GaSb-based semiconductor disk lasers," *IEEE J. Sel. Topics Quantum Electron.*, vol. 21, no. 6, pp. 324–335, Nov. 2015, doi: 10.1109/JSTQE.2015.2414919.

[14] P. Holl et al., "GaSb-based 2.0 μm SDL with 17 W output power at 20 °C," *Electron. Lett.*, vol. 52, no. 21, pp. 1794–1795, Oct. 2016, doi: 10.1049/el.2016.2412.

[15] J. Heidrich, M. Gaulke, B. O. Alaydin, M. Golling, A. Barh, and U. Keller, "Full optical SESAM characterization methods in the 1.9 to 3-μm wavelength regime," *Opt. Exp.*, vol. 29, no. 5, p. 6647, Mar. 2021, doi: 10.1364/oe.418336.

[16] J. Heidrich, M. Gaulke, M. Golling, B. O. Alaydin, A. Barh, and U. Keller, "324-fs pulses from a SESAM modelocked backside-cooled 2-μm VECSEL," *IEEE Photon. Technol. Lett.*, vol. 34, no. 6, pp. 337–340, Mar. 15, 2022, doi: 10.1109/LPT.2022.3156181.

[17] M. Gaulke, J. Heidrich, B. Özgür Alaydin, M. Golling, A. Barh, and U. Keller, "High average output power from a backside-cooled 2-μm InGaSb VECSEL with full gain characterization," *Opt. Exp.*, vol. 29, no. 24, p. 40360, Nov. 2021, doi: 10.1364/oe.438157.

[18] N. Huwyler, M. Gaulke, J. Heidrich, M. Golling, A. Barh, and U. Keller, "3-W output power from a 2-μm InGaSb VECSEL using a hybrid metal-semiconductor Bragg reflector," *Opt. Mater. Exp.*, vol. 13, no. 3, p. 833, Mar. 2023, doi: 10.1364/ome.485694.

[19] M. Gaulke et al., "Gigahertz semiconductor laser at a center wavelength of 2 μm in single and dual-comb operation," *Opt. Exp.*, vol. 32, no. 1, p. 26, Jan. 2024, doi: 10.1364/oe.503035.

[20] P. Tatar-Mathes et al., "Effect of non-resonant gain structure design in membrane external-cavity surface-emitting lasers," *IEEE Photon. Technol. Lett.*, vol. 35, no. 12, pp. 657–659, Jun. 15, 2023, doi: 10.1109/LPT.2023.3270404.

[21] D. Findlay and R. A. Clay, "The measurement of internal losses in 4-level lasers," *Phys. Lett.*, vol. 20, no. 3, pp. 277–278, Feb. 1966, doi: 10.1016/0031-9163(66)90363-5.

[22] S. Baumgärtner, H. Kahle, R. Bek, T. Schwarzbäck, M. Jetter, and P. Michler, "Comparison of AlGaInP-VECSEL gain structures," *J. Cryst. Growth*, vol. 414, pp. 219–222, Mar. 2015, doi: 10.1016/j.jcrysgro.2014.10.016.

[23] J. Paajaste, S. Suomalainen, R. Koskinen, A. Härkönen, M. Guina, and M. Pessa, "High-power and broadly tunable GaSb-based optically pumped VECSELs emitting near 2 μm," *J. Cryst. Growth*, vol. 311, no. 7, pp. 1917–1919, Mar. 2009, doi: 10.1016/j.jcrysgro.2008.10.071.